CASUALTY RISK ASSESSMENT OF UNCONTROLLED REENTRIES AFTER THE DEPLOYMENT OF THE FIRST LARGE SATELLITE CONSTELLATIONS

Carmen Pardini[(1)], Luciano Anselmo[(2)]

[(1)] ISTI-CNR, Via G. Moruzzi 1, 56124, Pisa, Italy, Email: Carmen.Pardini@isti.cnr.it
[(2)] ISTI-CNR, Via G. Moruzzi 1, 56124, Pisa, Italy, Email: Luciano.Anselmo@isti.cnr.it

ABSTRACT

From 2019 to 2024, the risk due to uncontrolled orbital reentries of spacecraft, upper stages, and large debris for people on the ground and commercial aircraft in flight was estimated using realistic models for the number and casualty area of the surviving fragments, and for the latitudinal distribution of population and planes in the air. Each reentered object was modeled independently, considering its correct orbital inclination. In addition, the effects of complete object demise below certain mass thresholds were also evaluated.

Although the reentry risks are still relatively small, they have grown considerably from 2019 to 2024, mainly due to increased space activities. In 2024, the collective casualty probability for people on the ground was between 4.5% and 9.8%, while the individual annual casualty probability was not more than 10^{-11}. Always in 2024, the likelihood of aircraft being impacted by fragments capable of causing a catastrophic failure was between 3×10^{-5} and 7×10^{-5}, corresponding, on average, to one airplane struck every 30,000 and 14,000 years, respectively. For commercial aircraft passengers, the collective casualty probability ranged from 0.42% to 0.84%, while the individual casualty probability was between 9×10^{-13} and 2×10^{-12}.

1 INTRODUCTION

Historically, the individual casualty risk on the ground due to uncontrolled reentries has been, and remains, extremely low compared to hazards commonly encountered in everyday life, not to mention many work activities. Even rare accidents like lightning strikes or shark attacks still pose a much greater risk. However, because of how they came into being, their profound media impact, and their inherently global nature, space activities have always been subject to the issue of safety, particularly of those not directly involved, that is, the general public. Therefore, the focus on public safety has always been very high globally, concentrating on collective rather than individual risk. It is in this context that the global casualty expectancy limit of 10^{-4} per uncontrolled reentry, as adopted by several national and international guidelines, standards, or laws, should be considered.

With this in mind, and also taking into account the growing attention to the possible risks to air traffic, which is characterized by very high safety standards and requirements, it is worth assessing what effect the recent increase in space activities, with the deployment of the first large satellite constellations, has had on the evolution of the casualty risk due to uncontrolled orbital reentries. This was the primary purpose of this paper, which analyzed the uncontrolled reentries of satellites, orbital stages, and sizable debris starting from a time before the launch of the first large constellations. The orbital inclination of the reentering objects and the time-varying average latitudinal distribution of the population on the ground were considered. To estimate the casualty expectancy of each event, three relationships from independent sources were applied, linking the dry mass of the object with the expected casualty area of the surviving fragments on the ground, allowing the consistency and dispersion of the results to be tested. In addition, different mass thresholds were applied to account for the fact that typical low-mass objects do not reach the Earth's surface and to estimate the beneficial impact of designing for complete demise.

Another issue this paper addresses is calculating the probability of uncontrolled reentering objects striking an aircraft. Although the likelihood of a direct impact with an airplane is still low, the increasing frequency of reentries may heighten the probability of close encounters. The expectation of collision with an aircraft was herein estimated for each reentry event that occurred during the period analyzed, and then the annual aggregate value was evaluated. Two different relationships were adopted to calculate the number of fragments per reentry event capable of causing catastrophic failure to an aircraft, and various mass thresholds were applied to account for the possible complete demise of objects below a certain mass.

This study confirms that the ground and airspace risk posed by uncontrolled reentries has increased significantly in recent years despite the growth in controlled reentries. However, a combination of generalized design for complete spacecraft demise and controlled reentries for massive orbital stages could be effective enough to avoid too rapid and significant an increase in casualty expectancy, at least during the early

Proc. 9th European Conference on Space Debris, Bonn, Germany, 1–4 April 2025, published by the ESA Space Debris Office
Editors: S. Lemmens, T. Flohrer & F. Schmitz, (http://conference.sdo.esoc.esa.int, April 2025)

phase of the mega-constellation era.

2 UNCONTROLLED REENTRIES

The analysis presented in this paper focused on uncontrolled reentries of human-made space objects that occurred between 2019 and 2024. The objects considered included satellites and orbital rocket stages classified as large – with a Radar Cross-Section (RCS) greater than 1 m^2 – and medium – with an RCS between 0.1 m^2 and 1 m^2 – by the US Space Surveillance Network (https://www.space-track.org). The reentering debris classified as large was also taken into account. The number of reentries per year and the annual returned mass were estimated from the beginning of 2019, the launch year of the first OneWeb and Starlink constellation satellites, to the end of 2024. For each reentered object, the final orbit before decay, along with other reentry information, was obtained from the Space-Track website (https://www.space-track.org), while the returned mass was acquired from the ESA's DISCOS database (https://discosweb.esoc.esa.int).

In addition to considering all objects mentioned above that fell within the period analyzed, regardless of their mass, two other classes of objects were assumed. One included only objects with a mass greater than 300 kg, and the other included only objects more massive than 600 kg. These mass thresholds were chosen to take into account the fact that typical low-mass objects might demise completely on reentry, thus preventing some fragments from reaching the airspace and the ground. For example, a lower mass threshold of 300 kg led to the exclusion of all first-generation Starlink satellites, with masses of 227 kg and 260 kg, as well as of many other small satellites, orbital stages, and debris.

2.1 All objects irrespective of their mass

From the beginning of 2019 to the end of 2024, almost 1731 artificial space objects – including satellites and orbital stages classified as medium and large and debris classified as large – have reentered the Earth's atmosphere without control. Of these, 69% were satellites, 24% were orbital stages, and 7% were large debris. These percentages changed significantly in 2024, bringing the contribution of satellites to 81%, against 15% for orbital stages and 4% for debris. The total mass returned uncontrolled from the beginning of 2019 to the end of 2024 was around 1361 metric tons. 67% of this mass was concentrated in orbital stages, 26% in satellites, and 7% in large debris. In 2024, the total returned mass was about 412 metric tons (57% more than in 2023), with a contribution of 55% from orbital stages, 39% from satellites, and 6% from large debris.

In summary, an average of 289 sizable objects per year reentered the Earth's atmosphere from the beginning of 2019 to the end of 2024, corresponding to 5-6 reentries per week. The average mass returned per year was about 227 metric tons, corresponding to about 4.4 metric tons per week. Focusing on 2024, the average number of reentered objects per week almost tripled (14 reentries) compared with the 2019-2024 average, while the weekly returned mass (about 8 metric tons) nearly doubled.

2.2 Objects with a mass greater than 300 kg

Of 1731 objects reentered without control in the six years considered (2019-2024), 587 had a mass greater than 300 kg. Orbital stages accounted for 53% of the reentries, followed by satellites with 33% and large debris with 14%. In 2024, the contribution to the reentry frequency increased to 51% for satellites, while it decreased to 39% for orbital stages and 10% for large debris. The total returned mass was about 1171 metric tons, meaning that objects lighter than 300 kg had a total mass of 190 metric tons. Out of 1171 metric tons, 77% belonged to orbital stages, 16% to satellites, and 7% to large debris. In 2024, 67% of the total returned mass was associated with orbital stages, 26% with satellites, and 7% with large debris.

Over the 2019-2024 period, about 98 objects with a mass greater than 300 kg reentered, on average, each year, corresponding to 1-2 objects per week. The mean mass returned annually was about 195 metric tons, corresponding to nearly 3.8 metric tons per week. In 2024, the average number of weekly reentries almost doubled (about 4 reentries) compared with the 2019-2024 average, while the mean mass returned exceeded 6 metric tons per week.

2.3 Objects with a mass greater than 600 kg

The 476 reentered objects with a mass greater than 600 kg had a total returned mass of about 1127 metric tons, meaning that objects between 300 and 600 kg had a total mass of 44 metric tons. Over the 2019-2024 period, the most significant contribution to the reentry frequency was due to orbital stages, accounting for 62% of the reentries, followed by satellites with 31%, and by large debris with 7%. The situation changed in 2024, when satellites accounted for 49% of the re-entries, followed by orbital stages (45%) and large debris (6%). Concerning the returned mass over the six years considered (1127 metric tons), 79% was concentrated in orbital stages, 15% in satellites, and 6% in large debris. In 2024, 69% of the total returned mass (313 metric tons) was associated with orbital stages, 25% with satellites, and 6% with large debris.

In 2019-2024, on average, about 79 objects with a mass greater than 600 kg reentered each year, corresponding to the reentry of 1-2 objects per week. The average annual mass returned was about 188 metric tons, corresponding to nearly 3.6 metric tons per week. In

2024, the number of weekly reentries almost doubled (about 3 reentries) compared with the 2019-2024 mean, while the mass returned was approximately 6 metric tons per week.

2.4 Overall picture

Summarizing the conclusions for the three groups of objects considered, from the beginning of 2019 to the end of 2024, the number of reentries without control varied from 5-6 per week for all objects to 1-2 per week for objects exceeding 300 or 600 kg. The average weekly returned mass ranged between 3.6 metric tons (objects with mass > 600 kg) and 4.4 metric tons (all objects), remaining around 4 metric tons for the three groups. Especially noteworthy was the situation that arose in 2024, which saw a considerable increase in reentries and the mass returned. The mean number of reentries grew to approximately 14 per week if all objects were considered, to 4 per week for objects with a mass greater than 300 kg, and 3 per week for objects exceeding 600 kg. The mean mass returned in 2024 ranged between 6 and 8 metric tons per week, almost doubling the 2019-2024 average.

Fig. 1 shows the number of uncontrolled reentries per year for the three groups of objects. Fig. 2 does the same for the returned mass. In Fig. 1, there is evidence of a considerable increase in the number of reentries that occurred in 2024, mainly represented by the numerous reentries from the Starlink constellation, accounting for nearly 57% of the total uncontrolled reentries of satellites in that year. In percentage terms, the increase was significant, although less marked, even limiting attention to objects more massive than 300 kg, ignoring the first-generation Starlink satellites.

Over the period considered, a substantial increase in the returned mass is evident in Fig. 2, mainly due to uncontrolled reentries of massive orbital stages. However, the contribution of satellites to the returned mass has grown significantly in 2024, reaching 39% of the total for all the objects and 25% for objects more massive than 600 kg.

Although this section highlighted the contribution of various typologies of objects, that is, satellites, orbital stages, and large debris, to the frequency of reentries and the mass returned, in the rest of the paper, and for the assessment of the risk on the ground and in the airspace posed by uncontrolled reentries, all objects as a whole will be considered, without dwelling on the contribution by type, which will instead be the subject of subsequent publications.

3 RISK ASSESSMENT ON THE GROUND

For an uncontrolled reentry, the main factors for assessing the risk of human casualties are the number and area of debris expected to reach the surface of the Earth, the kinetic energy of each surviving fragment, and the amount of the world's population potentially at risk. The latter depends on the orbital inclination of the reentering object and the year when the reentry occurs.

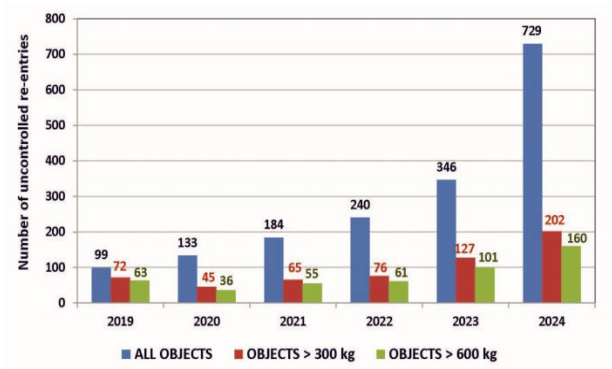

Figure 1. Annual number of uncontrolled reentries from 2019 to 2024

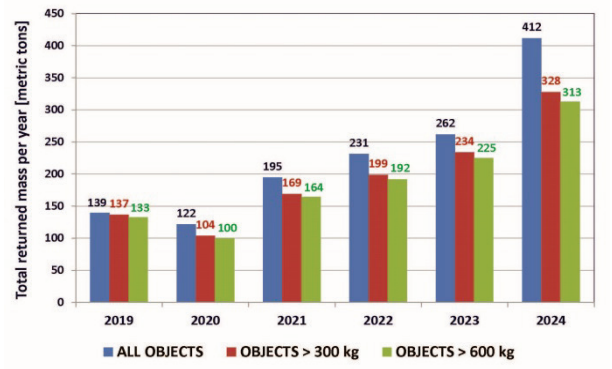

Figure 2. Annual returned mass from 2019 to 2024

According to the US Range Commanders Council (RCC) Standard 321-23 [1], a kinetic energy of 15 J represents the minimum impact energy for a potential injury (that is, when the impact causes sufficient harm to require an immediate level of professional medical care) to an unprotected person. Below this threshold, injury is highly unlikely to occur. Fatal injuries that fall under this standard, on the other hand, are those for which no medical intervention is possible and which are most likely to be lethal. As for [2], an energy threshold of 15 J corresponds to a probability of fatality of less than 0.05%, while probabilities of fatality of 1%, 50%, and 99% correspond to kinetic energies of 29 J, 103 J, and 359 J, respectively. Also, in the NASA Technical Standard 8719.14 [3], the potential for human casualty is assumed for any surviving fragment with an impact kinetic energy greater than 15 J. Moreover, for uncontrolled reentries compliant with the NASA standard requirement 4.7-1, human casualty risk from surviving fragments with impact kinetic energies greater than 15 J should be less than 0.0001 (1/10,000).

Several organizations and countries worldwide have endorsed and adopted this alert threshold. It was

included in the US Government *Orbital Debris Mitigation Standard Practices* [4] and is consistent with the casualty expectation for the general public from any single mission required by the US Range Commanders Council Standard 321-23 [1]. The same risk threshold was recommended by the Inter-Agency Space Debris Coordination Committee (IADC) [5], the European Space Agency (ESA) [6], the Japan Aerospace Exploration Agency (JAXA) [7], and several other space agencies and countries in the world, such as France, which transposed the standard into national law (https://www.legifrance.gouv.fr/loda/id/JORFTEXT000018931380).

For the evaluation of the human casualty expectation, also known as human casualty expectancy (E_C), the same formulation adopted by NASA in [3] was used in this paper, that is:

$$E_C = A_C \times P_D \tag{1}$$

where A_C represents the total debris casualty area, and P_D represents the total average population density in the latitude band overflown by the reentering object when reentry occurs.

3.1 Total debris casualty area

The formula adopted in [3] to compute the total debris casualty area (A_C) due to a reentry event is:

$$A_C = \sum_{i=1}^{N} \left(\sqrt{A_h} + \sqrt{A_i}\right)^2 \tag{2}$$

where N is the number of surviving fragments with impacting kinetic energy greater than 15 J, $A_h = 0.36$ m^2 is the average cross-sectional area of an exposed person – taken as the linear average of three distinct projected areas (standing, seated, prone) of an average human [3] – and A_i is the average cross-sectional area of each fragment surviving reentry.

Realistic estimates of the total debris casualty area for a reentry event require detailed information on the design and the materials the object under scrutiny is made of. Consequently, A_C values are only available for a limited subset of objects and often, even if known, are owned by various organizations and agencies, and typically are not publicly disclosed. Therefore, considering this parameter had to be evaluated for many reentry events, alternative, albeit coarser, methods had to be used to estimate it. In a previous work [8], several relationships for the A_C were obtained starting from the knowledge of the total debris casualty area available in the technical literature for a small sample of space objects (satellites and orbital stages), mostly already reentered, and then fitting the data with simple mathematical functions in terms of the dry reentering mass M. Among the various relationships obtained, the following was adopted in the present work to estimate the total debris casualty area:

$$A_C = 0.05627\, M^{0.7563} \tag{3}$$

where A_C is given in m^2 and M in kg.

Moreover, to check the consistency and dispersion of the results obtained, two other formulations for calculating the total debris casualty area were also considered, in addition to Eq. 3, referred to here as the ISTI relationship. Both formulations were found by ESA and were still based on a fit of historical reentry assessments for the debris casualty area as a function of dry reentering mass. The first, referred to here as ESA1, is described in [9], while the second, referred to as ESA2, in [10]. The ESA1 relationship is the following:

$$A_C = 14.58 + 14.59\, ln\, M \tag{4}$$

where A_C is expressed in m^2 and the reentering mass M is given in metric tons. The ESA2 formula is instead:

$$A_C = 5.6 \times M^{\frac{1}{4}} - 15 \tag{5}$$

where A_C is given again in m^2, but the reentering mass M is expressed in kg.

3.2 Casualty expectancy and probability

The world population potentially at risk is a function of both the inclination of the orbit of the reentering object and the year in which the reentry occurs. Suppose the expected number of casualties per unit casualty area is known as a function of orbit inclination and year. In that case, the casualty expectancy E_C (Eq. 1) can be obtained by multiplying this number by the total debris casualty area calculated using any of the Eqs. 3-5. In [8], the expected number of casualties per unit casualty area was available for the year 2020. Therefore, taking this case as a reference and considering the annual evolution of the world population (www.worldometers.info/world-population), the yearly percentages of decrease and increase were applied to the expected number of casualties per unit casualty area in 2020 to estimate the expected number of casualties per unit casualty area from 2019 to 2024 (Fig. 3).

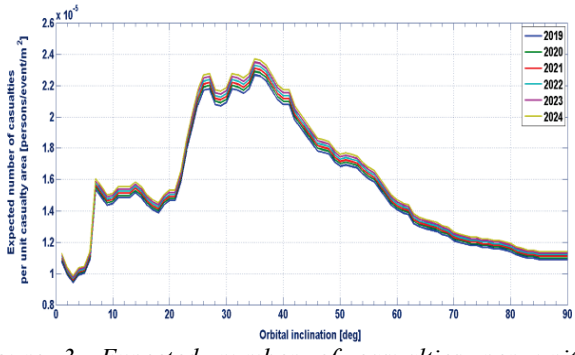

Figure 3. Expected number of casualties per unit casualty area as a function of orbital inclination and reentry epoch from 2019 to 2024

The casualty probability $P(k)$, where k represents the number of people injured or killed, was obtained from

the casualty expectancy E_C using the following Poisson distribution:

$$P(k) = \frac{{E_C}^k \times e^{-E_C}}{k!} \quad (6)$$

Then, the probability of having no casualties ($k = 0$) was given by:

$$P(0) = e^{-E_C} \quad (7)$$

while the probability of having one or more casualties was obtained by:

$$P(k \geq 1) = 1 - e^{-E_C} \quad (8)$$

3.3 Risk for unsheltered people on the ground posed by uncontrolled reentries from 2019 to 2024

Eqs. 3-5 were applied to the 1731 uncontrolled reentries of human-made space objects from 2019 to 2024 to compute the total debris casualty area per reentry event. Fig. 4 shows the casualty area in terms of the returned mass obtained with the three relationships. In addition to the plots that refer to all masses under consideration, including those over 20 metric tons associated with the reentry of some large Chinese orbital stages, two zoomed views, between 0 and 7000 kg and between 0 and 600 kg, are shown as well, to highlight the trends for smaller masses.

For the two ESA formulations, there is a mass threshold below which the object under scrutiny would have a negative casualty area and, then, would not present a reentry risk. This cut-off mass is around 370 kg – thus excluding, among others, all first-generation Starlink satellites – for Eq. 4 (ESA1) and around 50 kg for Eq. 5 (ESA2). Note that each single point in the figure may represent many objects with the same returned mass.

The total debris casualty area per year and formula is presented in Fig. 5. From 2019 to 2024, overall, it was 20,430, 20,908, and 26,797 m^2 for the ISTI, ESA1, and ESA2 relationships, respectively. The ESA2 formula generally obtained a higher total casualty area than the other two, especially during 2024, characterized by the reentry of numerous satellites. However, having obtained the three formulations from different groups of objects (satellites and orbital stages), it is still surprising how good the agreement was.

In addition, as anticipated in Section 2, to account for the fact that objects below a certain mass threshold might completely demise upon reentry, and thus, no fragments would survive to reach the ground, two other subsets of reentered objects were considered. One included all objects above 300 kg (587 objects), and the other included those above 600 kg (476 objects). Eqs. 3-5, and the subsequent analysis, were applied to these two subsets of objects as well. In the following, for clarity, ISTI All, ESA1 All, and ESA2 All refer to the complete set of 1731 reentering objects, while ISTI 300, ESA1 300, and ESA2 300 refer to the objects more massive than 300 kg, and ISTI 600, ESA1 600 and ESA2 600 to those with a mass exceeding 600 kg.

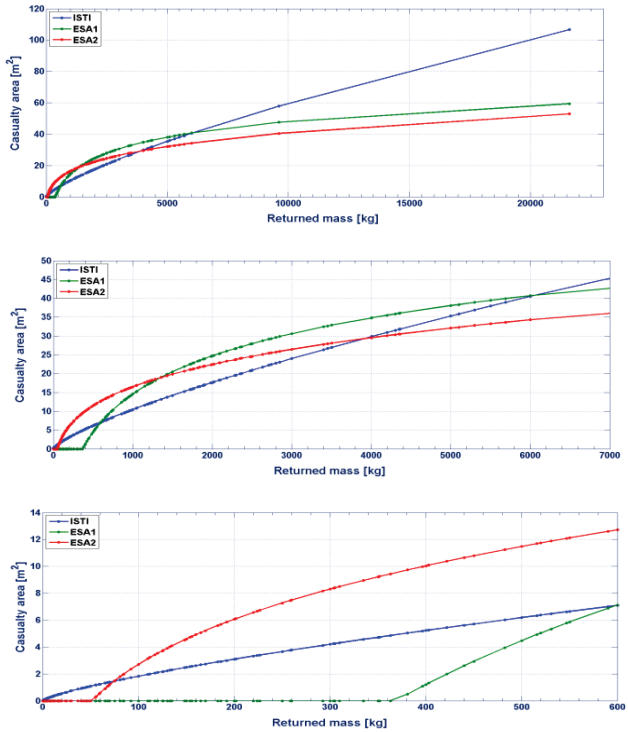

Figure 4. Casualty area versus mass computed for objects reentered uncontrolled from 2019 to 2024, using Eq. 3 (ISTI), Eq. 4 (ESA1), and Eq. 5 (ESA2); the top figure shows all ranges of masses up to more than 20 metric tons, the intermediate figure is for masses up to 7 metric tons, while the bottom one is up to 600 kg

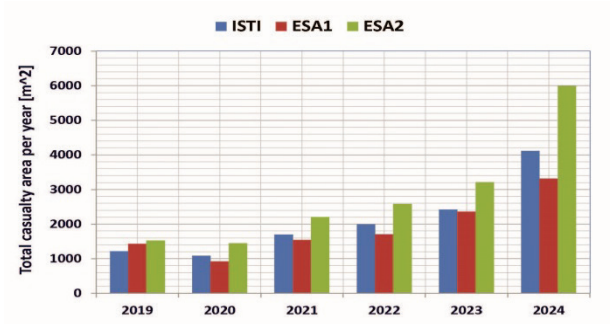

Figure 5. Total debris casualty area per year computed with the ISTI, ESA1, and ESA2 relationships for the 1731 uncontrolled reentry events that occurred from 2019 to 2024

At this point, for each uncontrolled reentry event from 2019 to 2024, belonging to the three sets with different lower mass thresholds (0, 300, and 600 kg), the total debris casualty area obtained with each formulation (Eqs. 3-5) was multiplied by the expected number of

casualties per unit casualty area (Fig. 3) – a function of both the orbital inclination of the reentering object and the year in which its reentry occurred – to estimate the casualty expectancy associated with each reentered object. The total casualty expectancy (E_C) per year was calculated by summing the casualty expectancy for each object reentered that year. It should be noted that E_C is not the probability of casualty. As a matter of fact, the casualty expectancy may be greater than one in unusual situations, while the probability of casualty can never be. Here, the probability of casualty per year was obtained as a function of the corresponding annual E_C value using Eq. 8.

The annual casualty expectancy for the nine cases analyzed, resulting from three formulations to compute A_C (ISTI, ESA1, and ESA2) and three different lower threshold masses (0, 300, and 600 kg), is given in Fig. 6 and refers to people in the open. It represents the "collective risk", that is the expected number of casualties anywhere in the world. It ranged between approximately 0.02 (one mean casualty every 50 years) in 2019 for all formulations and 0.10 (one mean casualty every 10 years) in 2024 for the ESA2 All case. Always in 2024, the values of E_C varied from 0.07 (ISTI All) to 0.06 (ESA1 All, ESA1 300, ESA1 600, ESA2 300, ESA2 600), and 0.05 (ISTI 300, ISTI 600), with one casualty expected, on average, every 14, 17 and 20 years, respectively.

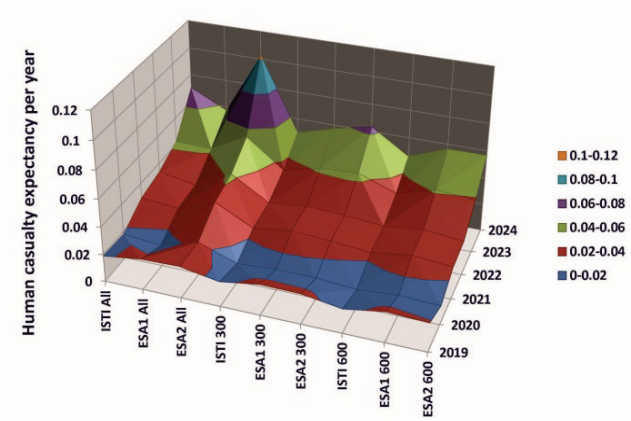

Figure 6. Human casualty expectancy per year due to uncontrolled reentries from 2019 to 2024, as a function of the formulation used to estimate A_C and the lower mass threshold applied to reentering objects

To guess the annual individual casualty expectancy, that is, the average "individual risk" of injury for any particular person, the global casualty expectancy should be divided by the number of inhabitants on the ground each year. Considering that the world's population has increased from about 7.8 billion people in 2019 to about 8.2 billion people in 2024, the situation for all nine cases is shown in Fig. 7. With most formulations, the individual annual casualty expectancy exceeded 5×10^{-12} since 2023, reaching a maximum of the order of 10^{-11} in 2024 (ESA2 All). Hence, uncontrolled reentries still present an extremely low risk for any single specific individual, compared with other risks faced in everyday life, but the average value calculated from the nine cases in 2024 was about three times higher than that obtained in 2019. Therefore, what matters is not the value of the risk itself recorded to date but the possibility that this risk will increase considerably in the near future if appropriate mitigation measures are not taken.

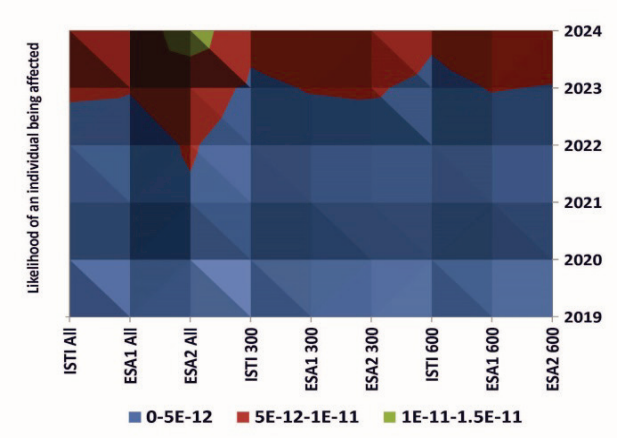

Figure 7. The likelihood of any specific individual being injured by fragments of uncontrolled reentries from 2019 to 2024, as a function of the year and the formulation adopted to compute A_C

For people in buildings or shelters, the total debris casualty area of surviving fragments from reentering objects may be greater or smaller than that computed in Eq. 2. The exact outcome depends on the fragment's capability to penetrate and gravely damage the sheltering structure, on the excess kinetic energy retained by the impactor if penetration occurs, and on the falling structural debris produced by the impact [11]. As such, the human casualty risk associated with uncontrolled reentry can be subdivided into primary and secondary [12]. The primary risk derives from the possibility of a direct hit of people in the open by falling debris. The secondary risk is instead associated with a potential debris impact on a building, a shelter, a high-risk industrial plant, or a vehicle, such as an aircraft, ship, or train, possibly leading to indirect human casualties. While the primary risk can be evaluated using Eqs. 1-2, there is no easy way to compute the secondary risk because a relatively minor impact might be associated with potentially catastrophic consequences in certain unfavorable circumstances. However, in [12] and [3], it was concluded that considering all the uncertainties underlying the computation of A_C, the equations used to assess the casualty expectancy and probability for people in the open should also provide a correct order of magnitude for sheltered people.

The annual global casualty probability, computed with

Eq. 8 for the nine cases analyzed, is shown in Fig. 8. Note that the cases reported are eight instead of nine because ESA1 All coincides with ESA1 300 due to the cut-off mass in the ESA1 formulation, which excludes all objects with a mass lower than 300 kg. The usefulness of Fig. 8 lies in showing the range of variation for the global casualty probability over the years. A significant growth over time is evident in all cases. The maximum increase is observed for the ESA2 All formulation (Eq. 5 applied to the 1731 reentry events irrespective of their mass), leading to a global casualty probability of 9.8% in 2024. The minimum increase is associated with the ISTI 600 formulation (Eq. 3 applied to the 476 reentered objects with mass greater than 600 kg), with a casualty probability of 4.5% in 2024.

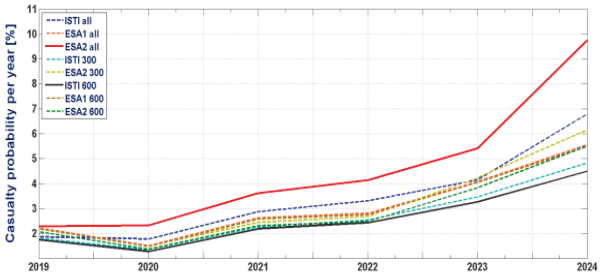

Figure 8. Global casualty probability per year for the nine cases analyzed, with three formulations to compute A_C and three different lower cut-off masses

The information drawn from Fig. 8 is that, in 2024, the likelihood of having, around the world, at least one generic person injured on the ground because of uncontrolled reentries was not less than 4.5%, even assuming that for reentering objects under 600 kg there were no fragments capable of reaching the surface of the Earth. On the other hand, it cannot be excluded that the global casualty probability may have approached 10% if no reentered object was completely demised and Eq. 5 fitted the casualty area better. From 2019 to 2024, based on Fig. 8, the global casualty probability ranged between 1.7% and 2.3% in 2019, 1.3% and 2.3% in 2020, 2.2% and 3.6% in 2021, 2.4% and 4.1% in 2022, 3.3% and 5.4% in 2023, and 4.5% and 9.8% in 2024.

Fig. 9 shows the global casualty probability computed for each formulation used to assess A_C (ISTI, ESA1, and ESA2) as a function of the three different lower mass thresholds for complete demise, that is, 0, 300, and 600 kg. Concerning the ESA1 formulation, the values of the global casualty probability in the intermediate figure are practically the same, irrespective of the mass threshold, because Eq. 4 already neglects the contribution of objects less massive than approximately 370 kg (Fig. 4). Then the cases ESA1 All and ESA1 300 are nearly identical. The relatively small number and total mass of objects between 300 and 600 kg do not change the result much for ESA1 600. Instead, marked differences can be seen with the ISTI (top of Fig. 9) and ESA2 (bottom of Fig. 9) formulations. Focusing on 2024, the global casualty probability for the ISTI formulation decreased from 6.8% to 4.5% if objects lighter than 600 kg were supposed to demise upon reentry completely. Instead, it reduced to 4.8% if only objects lighter than 300 kg fully demised. Concerning the ESA2 formulation, the global casualty probability reduced from 9.8% to 5.5% if objects lighter than 600 kg were considered fully demisable, and to 6.1% if the same was true only below 300 kg.

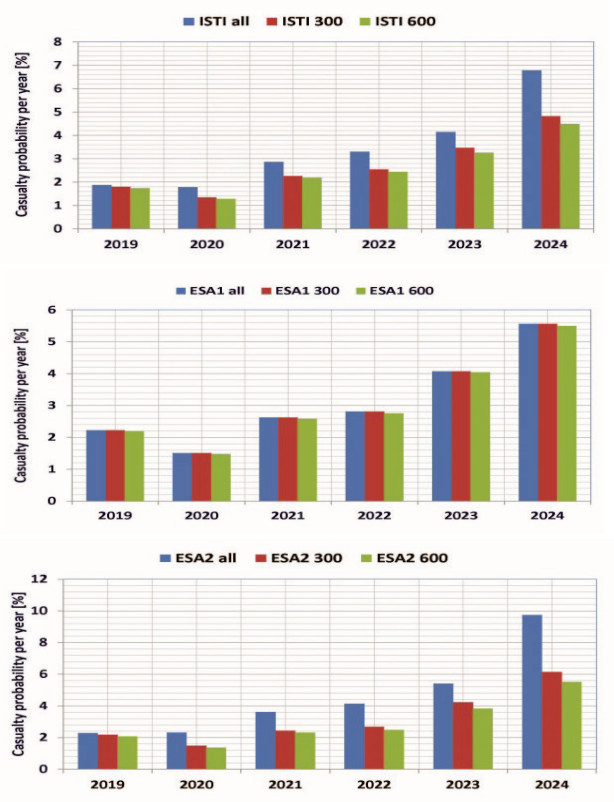

Figure 9. Global casualty probability per year associated with uncontrolled reentries from 2019 to 2024. From top to bottom, the figure shows the results obtained with the three formulations to compute A_C as a function of the three different lower mass thresholds

Comparing the three formulations for each group of objects, the largest, though relatively small, differences were observed when all reentry events were considered (Fig. 10). In such a case there was better agreement between the ISTI and ESA1 formulations, while ESA2 provided systematically higher values from 2020 onward (top of Fig. 10). The agreement was very good for objects more massive than 300 kg (middle of Fig. 10), with consistently lower ISTI values, and a similar behavior was observed for objects above 600 kg (bottom of Fig. 10). A perspective view of the global casualty probability per year is given in Fig. 11, in terms of the formulation adopted to compute A_C and the cut-off masses.

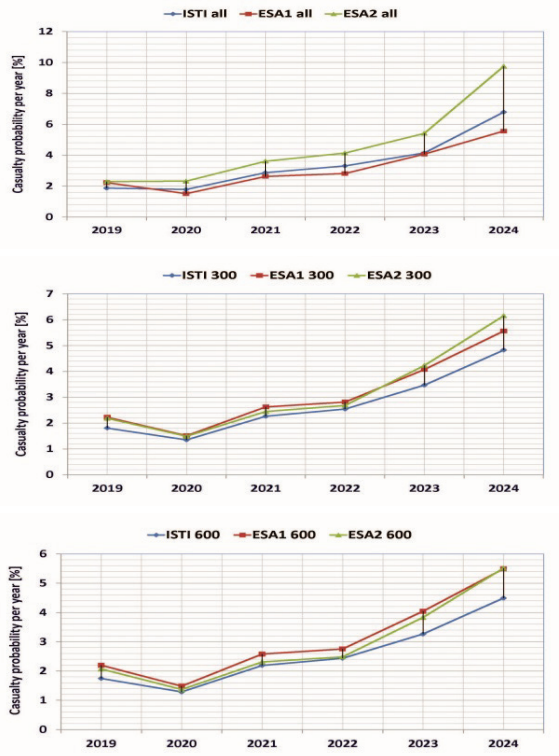

Figure 10. Comparison of the annual global casualty probability using Eqs. 3-5 with the three different lower cut-off masses (0 kg top, 300 kg middle, 600 kg bottom)

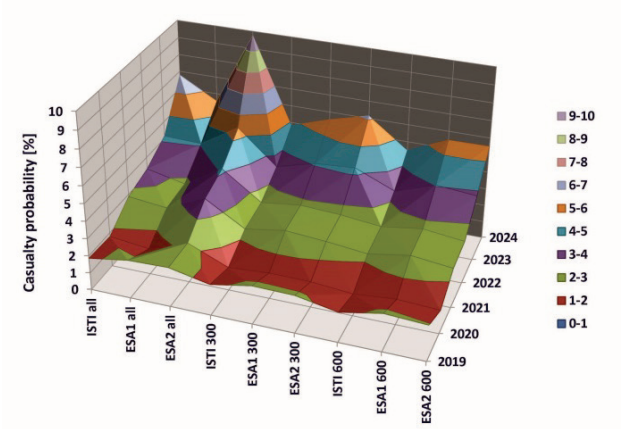

Figure 11. Global casualty probability per year for the three formulations to compute A_C and the three different lower cut-off masses

4 RISK ASSESSMENT FOR AIRCRAFT

For airplanes in flight, moving around at several hundreds of kilometers per hour, the problem is quite different because even the impact with debris practically at rest in the air could have severe consequences for the passengers on board [11,12]. The consequences of fragments impacting aircraft range from insignificant to catastrophic. Fragment mass, shape, material, impact velocity vector, aircraft type, location, and impact geometry are among the major factors determining consequences [1]. A key assumption made by all aircraft vulnerability models approved by the US Range Commanders Council is that any impact of fragments with a mass greater than 300 g anywhere on the aircraft can produce a catastrophe. This case could lead to an uncontrolled landing that may result in multiple casualties, typically with the loss of the plane [13]. But also pieces of metal as small as 0.5 g (tungsten) or 1 g (steel and aluminum) could critically damage windshields or engines, sometimes leading to aircraft loss [1].

Various investigations have been conducted concerning the risk of falling debris on aircraft since 2008 [12,14–19]. Also, the International Association for the Advancement of Space Safety (IAASS) devoted a chapter in [20] to the risk for aircraft from launch and reentry operations, presenting methods to assess the risk, evaluate the aircraft vulnerability, and propose risk mitigation strategies.

The seminal Patera's analysis conducted in 2008 [15] was based on data from 17 of the most popular commercial aircraft with departures or destinations in the United States while also considering the in-flight time of each aircraft type in 2006. The study assumed 100 reentries of large objects per year and 100 hazardous fragments per reentry event, bringing the number of objects per year that might threaten an aircraft to 10,000. Under these assumptions, the annual worldwide probability of a commercial aircraft being struck by falling debris was expected to be on the order of 3×10^{-4}, or one event every approximately 3300 years, on average.

More recently, the US Federal Aviation Administration (FAA) sponsored a study performed by The Aerospace Corporation to assess the risk for people on the ground and aboard aircraft due to falling debris from low Earth orbit constellations [17]. The analysis made projections through 2035, considering plans to put large satellite constellations into orbit in the next decade. Global air traffic was projected until 2035, assuming that fragments capable of causing ground casualties were also capable of fatally damaging an aircraft. It was found that the probability of an aircraft being struck by a hazardous fragment was 8.4×10^{-6} in 2021 and would reach 7.0×10^{-4} in 2035.

The analysis conducted in this paper starts from some of the general assumptions considered in The Aerospace Corporation study [17], with a specific focus on the expectancy of aircraft impact per debris object estimated in 2021, as shown in figure 16 on page 29 of [17]. This collision expectancy, represented as a function of the orbital inclination of the reentering object and the reentry time, was estimated in [17] by multiplying the average aircraft exposed area by the air traffic density per latitude and the probability of object reentry per

latitude. The mean aircraft surface that could be impacted by reentering debris – the mean exposed vulnerable surface area – was estimated in [21] based on an average performed on all commercial aircraft typically in flight, and was found to be 1150 m^2. Based on this, the mean aircraft vulnerable exposed area considered in [17] and the present study was assumed to be 1000 m^2.

4.1 Expectancy of commercial aircraft impact per debris object

To obtain the expectancy of a commercial aircraft strike per debris object from 2019 to 2024, the collision expectancy available in 2021, given in figure 16 (page 29) of [17], was multiplied by a factor considering the different number of commercial flights in the period analyzed. According to [22], the number of commercial flights grew steadily from the 2000s until 2019, when it reached 38.9 million. However, due to the coronavirus pandemic, it fell to 18.3 million in 2020, then rose again in subsequent years to a projected value for 2024 comparable with that in 2019 (Fig. 12). Thus, compared with 2021 [22], the multiplicative factor was about: 1.9 for 2019, 0.9 for 2020, 1.0 for 2021, 1.4 for 2022, 1.7 for 2023, and 1.9 for 2024.

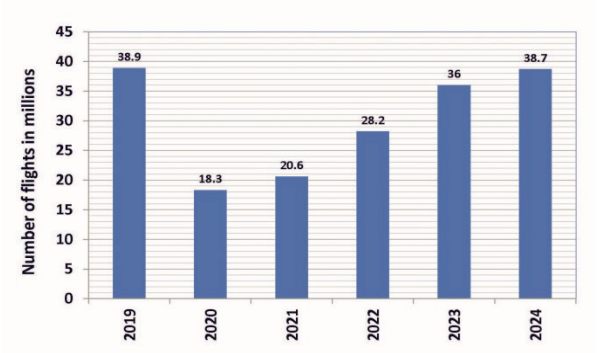

Figure 12. Number of commercial flights from 2019 to 2024

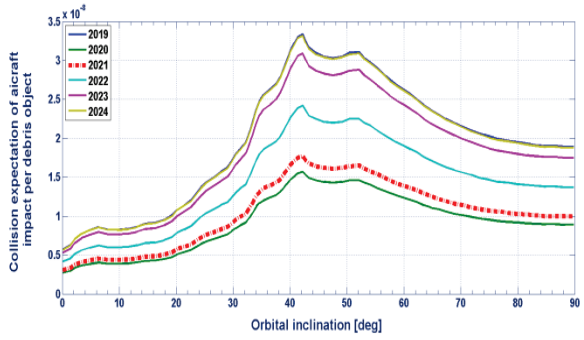

Figure 13. Expectancy of an aircraft impact per debris object from 2019 to 2024 as a function of the reentry orbital inclination

Fig. 13 shows the expectancy of an aircraft impact per debris object as a function of the orbital inclination of the reentering object and the year. For example, for an object reentered from an orbit with an inclination of 50 degrees, such collision expectancy was 1.46×10^{-8} if the reentry occurred in 2020 and 3.08×10^{-8}, which is twice as much if the reentry happened in 2024. With an inclination of 80 degrees, it was 9.17×10^{-9} for a reentry occurred in 2020, and 1.94×10^{-8} for a reentry in 2024. These results are in good agreement with the simplified analysis presented in [12].

4.2 Expectancy of an aircraft impact per reentry event

Each reentry event can generate several fragments that can survive, cross the airspace, and reach the ground. Fragments of mass greater than 300 g striking an aircraft can cause a catastrophic failure in which every passenger on board is a casualty. The expectancy of an aircraft impact per reentry event was obtained in this paper by multiplying the expectancy of an aircraft impact per debris object by the number of fragments hazardous to aircraft generated by that event.

4.3 Number of fragments per reentry event able to cause an aircraft catastrophic failure

The challenge was finding the number of debris hazardous to aircraft for each uncontrolled reentry event from 2019 to 2024. For the risk on the ground, the total debris casualty area was expressed in terms of the dry mass reentering, as in Eqs. 3-5, where the relationships were obtained based on available A_C values as a function of mass for a sample of satellites and orbital stages [8]. Here, using a similar approach, the number of fragments N capable of causing an aircraft catastrophic failure, that is, those with a mass greater than 300 g, was derived for the same sample of objects considered in [8], with the exclusion of the Compton Gamma Ray Observatory, for which N was not available. Tab. 1 lists the objects considered, along with the reentering dry mass M, the number of fragments N more massive than 300 g, potentially hazardous to aircraft [13], and the software tool used to estimate this number in the simulated cases.

Because of the smallness of the sample and the data properties, the values of N listed in Tab. 1 were fitted as a function of the reentering dry mass M by minimizing the absolute difference of the residuals (LAR) with two simple linear functions. The first fit, which we will refer to from now on as LIN1, included all the objects in the sample and is given by:

$$N = 0.0068 \times M \tag{9}$$

where the dry mass M is expressed in kg. However, since in the available data (Tab. 1) there was only one isolated object of very high mass, the HST of about 12

metric tons, while all the others were distributed between 200 and 6000 kg, the least absolute residuals (LAR) linear fit was also done excluding the most massive object. This second relationship, which we will refer to from now on as LIN2, is given by:

$$N = 0.0046 \times M \quad (10)$$

where the dry mass M is again expressed in kg.

Table 1. Number of surviving fragments more massive than 300 g – potentially hazardous to aircraft – for a sample of reentering satellites and orbital stages

Object	*M* [kg]	*N*	Model
PAM-D/STAR-48B	230	1	(*)
Test-Sat	400	3	SCARAB
Iridium (1st gen.)	560	6	ORSAT
Delta 2nd Stage	800	6	(*)
GOCE	1034	33	SCARAB
BeppoSAX	1386	33	SCARAB
EOS-Aura	2400	9	ORSAT
ROSAT	2426	15	SCARAB
TRMM	2621	12	ORSAT
GPM	2676	30	ORSAT
EUVE	3243	9	ORSAT
GLAST/Fermi	3639	14	ORSAT
Terra	4427	30	ORSAT
UARS	5668	26	ORSAT
HST	11,792	100	ORSAT

**Estimate based on recovered debris*

Applying both relationships to all reentry events from 2019 to 2024, the range of variation in the number of hazardous objects for aircraft, as a function of the reentering mass, is shown in Fig. 14. The upper figure shows the calculated numbers for all reentry events, from 2019 to 2024, thus including massive objects up to more than 20 metric tons. The middle figure zooms in on reentering masses up to 7000 kg, while the lower figure does the same for masses up to 600 kg. For example, if the reentering dry mass is about 5000 kg, the number of potentially harmful fragments may vary between 23 and 34, while if the mass is 500 kg, it may vary between 2 and 3.

Fig. 15 shows the total number of objects hazardous to aircraft per year, computed for all the 1731 reentry events considered in this paper (see Section 2). Note that this number increased from 948 in 2019 to 2800 in 2024, using Eq. 9 (LIN1) and from 641 to 1895 with Eq. 10 (LIN2), almost tripling in 2024 compared with 2019. If Eqs. 9 and 10 are applied to reentered objects with mass greater than 300 and 600 kg (see Section 2), then the annual range of values of N is shown in Fig. 16. LIN1 All and LIN2 All refer to the application of Eqs. 9 and 10 to all reentering objects, irrespective of their mass, LIN1 300 and LIN2 300 to objects with mass greater than 300 kg (587 objects), and LIN1 600 and LIN2 600 to objects exceeding 600 kg (476 objects).

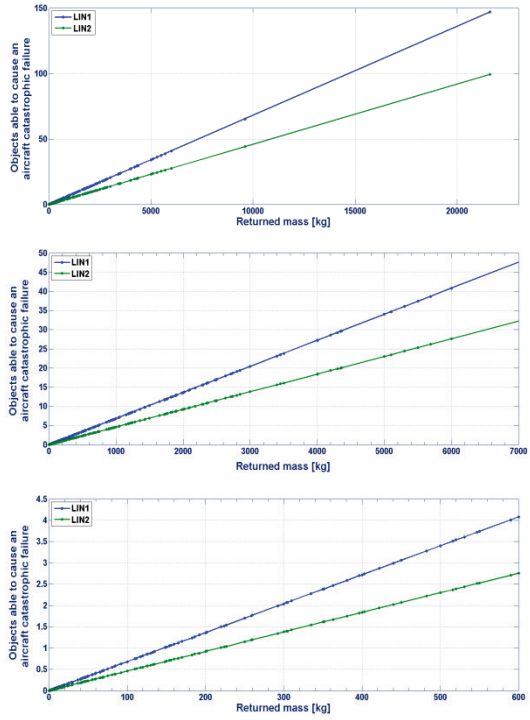

Figure 14. Number of objects capable of causing an aircraft catastrophic failure, as a function of the reentering mass, obtained with the two relationships LIN1 and LIN2

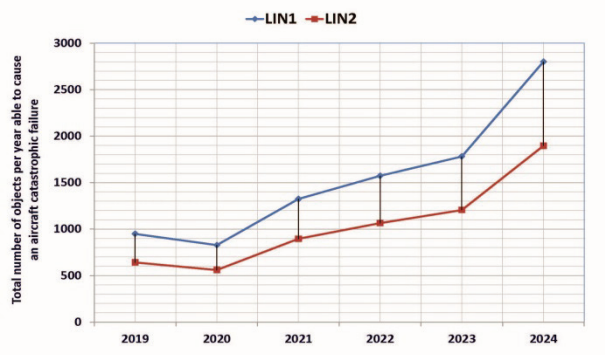

Figure 15. Total annual number of debris hazardous to aircraft computed with Eqs. 9 (LIN1) and 10 (LIN2) for the 1731 uncontrolled reentries occurred from 2019 to 2024

Fig. 16 shows that regardless of the relationship used to calculate the number of fragments and the lower mass

threshold considered, in 2023 the number of fragments from uncontrolled reentries potentially hazardous to aircraft was between 1000 and 2000. In 2024, this number further increased to more than 2000, but less than 3000, when using Eq. 9. These numbers are in any case relatively lower than those assumed in [15], that is, 10,000 harmful fragments in 2006, but are fairly consistent with those reported in [17] for the year 2021, that is 700 dangerous fragments (see also Fig. 15).

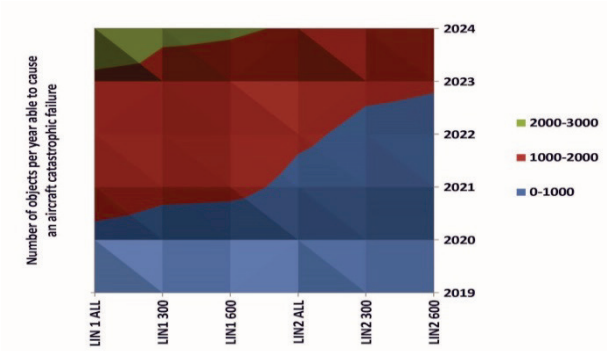

Figure 16. Total annual number of objects hazardous to aircraft computed with Eqs. 9 (LIN1) and 10 (LIN2), and three different lower mass thresholds for reentered objects (0, 300, and 600 kg)

4.4 Expectancy of an aircraft strike due to uncontrolled reentries from 2019 to 2024

The expectancy of a hazardous aircraft impact for each uncontrolled reentry from 2019 to 2024 was calculated as explained in Section 4.2. Then, for each year, the cumulative collision expectancy was obtained by summing the contributions of all reentry events in that year. The cumulative collision expectancy per year (E_a) of an aircraft being hit by a hazardous fragment from a reentry occurring in that year is shown in Fig. 17. It ranged from a minimum of 5.4×10^{-6} (LIN2 600 in 2020) to a maximum of 7.0×10^{-5} (LIN1 All in 2024). This means that, even in the worst case (LIN1 All in 2024), we can expect about one catastrophic collision with an aircraft every 14,000 years, on average.

This is a much more optimistic situation than that presented in [15] for 2006. The difference is probably primarily due to the number of potentially damaging objects for an aircraft. While in this work, based on actual reentries and fits of resulting hazardous fragments, the maximum annual value obtained was 2800 hazardous fragments in 2024 (with LIN1 All), in [15] the number of dangerous fragments was assumed to be 10,000 in 2006. However, comparing the results obtained in this paper with a more recent analysis [17], it was found that in 2021 (the year in which results were available in [17] as well), the likelihood of an aircraft being hit by hazardous reentering debris ranged in this paper from 1.0×10^{-5} (LIN2 600) to 1.8×10^{-5} (LIN1 All), against 8.4×10^{-6} obtained in [17]. The slightly higher values found in this paper were likely mainly due to a larger number of dangerous fragments, between 756 and 1324 for 2021, versus the 700 estimated in [17].

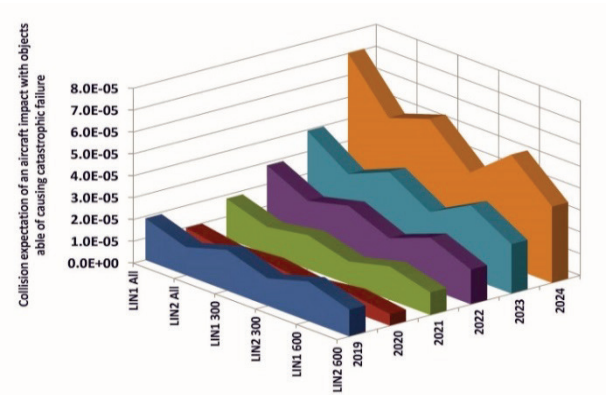

Figure 17. Total annual expectancy of an aircraft being struck by fragments capable of causing its catastrophic failure as a function of the lower threshold mass of reentering objects and the relation used to estimate the number of fragments

4.5 Collective casualty expectancy for aircraft passengers

Assuming an average of 120 passengers per aircraft in flight [17], the collective annual human casualty expectancy for passengers on board (E_{ap}) was obtained by multiplying 120 by the annual catastrophic collision expectancy for aircraft (E_a). Fig. 18 shows the passenger casualty expectancy per year as a function of the relation used to compute the number of fragments hazardous to aircraft and the lower mass threshold of reentering objects. In 2024, it ranged between 4.2×10^{-3} (LIN2 600) and 8.4×10^{-3} (LIN1 All). In 2021, it ranged between 1.2×10^{-3} (LIN2 600) and 2.2×10^{-3} (LIN1 All). Always in 2021, it was found to be 1.0×10^{-3} in [17].

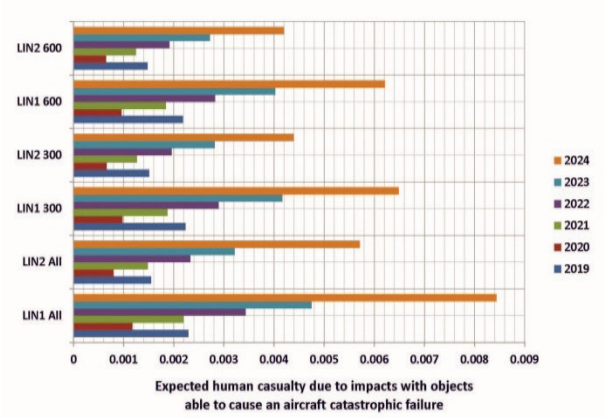

Figure 18. Passenger casualty expectancy per year as a function of the relation used to estimate the number of dangerous fragments and the lower mass threshold of reentering objects

4.6 Individual casualty expectancy for aircraft passengers

The annual individual casualty expectancy for a single passenger on board an aircraft can be roughly estimated, on average, by dividing E_{ap} by the number of passengers each year. The number of flying passengers from 2019 to 2024 is given in Fig. 19 [22]. It dropped from 4543 million passengers in 2019 to 1757 million in 2020 due to the coronavirus pandemic but then rebounded to 4964 million passengers projected in 2024. Fig. 20 shows the annual individual casualty expectancy for a single passenger from 2019 to 2024. Overall, it ranged from 3.3×10^{-13} and 1.7×10^{-12}. In 2024, it was between 8.5×10^{-13} (LIN2 600) and 1.7×10^{-12} (LIN1 All).

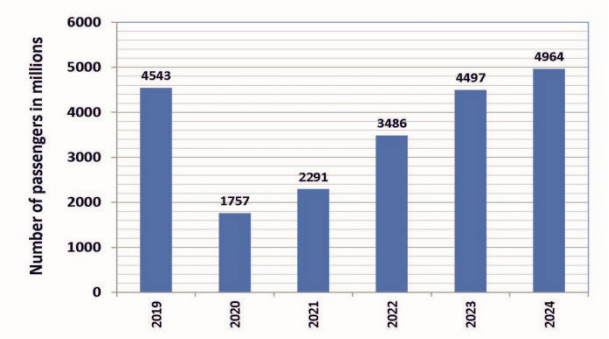

Figure 19. Annual number of passengers flown, from 2019 to 2024, aboard commercial aircraft

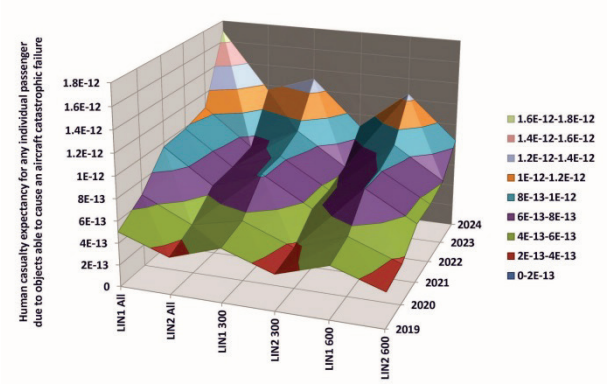

Figure 20. Individual casualty expectancy for a single aircraft passenger from 2019 to 2024, as a function of the relation used to estimate the number of dangerous fragments and the lower mass threshold of reentering objects

4.7 Probability of aircraft being impacted by dangerous fragments and collective casualty probability for passengers

The annual probability P_a of aircraft being impacted by fragments capable of causing their catastrophic failure was calculated from the cumulative yearly collision expectancy (E_a) as:

$$P_a = 1 - e^{-E_a} \tag{11}$$

Since the values of E_a are quite low, $P_a \approx E_a$. Therefore, Fig. 17 can also represent the probability of one or more aircraft being impacted by hazardous fragments.

As for the collective casualty probability for passengers on board (P_{ap}), Eq. 11 was still used by replacing E_a with E_{ap}:

$$P_{ap} = 1 - e^{-E_{ap}} \tag{12}$$

This probability is summarized in Fig. 21. Part of the differences found year after year is obviously due to the fluctuations in air traffic (Fig. 12) and passengers carried (Fig. 19) due to the coronavirus pandemic, with a significant drop in 2020, compared with 2019, and the subsequent stable recovery. However, the most striking aspect of Fig. 21 is the considerable difference in the collective aircraft passenger casualty probability found between the year 2019 and the year 2024, in which the number of commercial flights and passengers was virtually the same. In fact, in 2024, the collective passenger casualty probability, depending on the relation used to estimate the number of dangerous fragments and the lower mass threshold of reentering objects, ranged from 0.42% (LIN2 600) to 0.84% (LIN1 All), that is values between 3 and 4 times higher than those found for 2019. This impressive increase is attributable to the rapid growth of space activities and uncontrolled reentries from 2019 to 2024, as shown in Figs. 1 and 2.

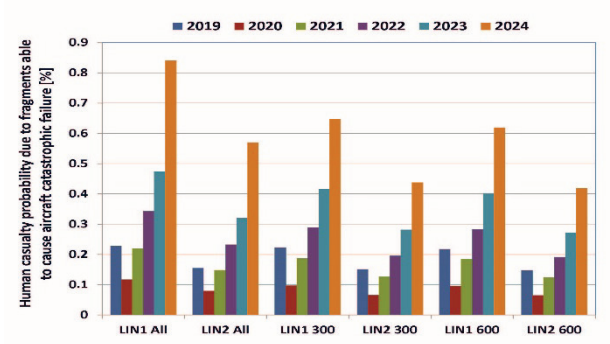

Figure 21. Collective casualty probability for aircraft passengers as a function of the relation used to estimate the number of dangerous fragments and the lower mass threshold of reentering objects

As for people on the ground, even for passengers on commercial flights the risk posed by uncontrolled orbital reentries, while not insignificant, is still small compared to the risks we face daily, collectively and individually. But the very rapid increase seen from 2019 to 2024, combined with the expected substantial growth of commercial air traffic and the boom of orbital activities related to the new space economy, is a serious source of concern for the future, requiring appropriate and effective mitigation measures to be taken before it is too late.

5 CONCLUSIONS

From 2019 to 2024, the number of uncontrolled reentries of spacecraft, orbital stages, and large debris increased by more than a factor of 7, while the returned mass increased by a factor of 3. Even if the attention was limited to objects more massive than 300 or 600 kg, the increments in number and mass were between 2 and 3 times. This affected the risks posed by these events to people on the ground and to air traffic.

Concerning the collective casualty risk for people on the ground, evaluated following the recommendations of the NASA standard [3], the total casualty area of each reentry event was estimated with three relationships, one from ISTI-CNR and two from ESA, based on data from detailed simulations and recovered debris. To assess the consequences of complete object demise during reentry below specific mass values, the analysis was applied to three sets of reentered objects, with different lower mass thresholds of 0 kg (all objects considered), 300 kg, and 600 kg.

The collective casualty probability for people on the ground was around 2% in 2019, with all three relationships and mass thresholds. Still, it increased in 2024, with values between 4.5% (ISTI 600) and 9.8% (ESA2 All). Regarding the corresponding individual annual casualty probability, in 2024 it was not more than 10^{-11}. Thus, uncontrolled reentries still present a very low collective and individual risk on the ground compared with other hazards faced in everyday life, but the values are growing fast, more than doubling between 2019 and 2024.

The risk for commercial aircraft and passengers was analyzed as well, using the approach outlined in [12] and detailed in [17]. This work's main novelty was using two ISTI-CNR relations, based on data from detailed simulations and recovered debris, to estimate – for each reentry event – the number of fragments potentially leading to an aircraft catastrophic failure in case of impact. In other words, the fragments potentially dangerous for aircraft were not set a priori, as in previous studies [15–19], but calculated for each actual reentry that occurred with the two ISTI-CNR relations as a function of the mass of the reentering object. Also, in this case, to assess the effects of complete object demise below specific mass values, the analysis was applied to three sets of reentered objects with different lower mass thresholds of 0 kg (all objects included), 300 kg, and 600 kg.

The results obtained, highly dependent on the number of fragments potentially dangerous to aircraft assumed or calculated, found risk figures that were relatively lower than those mentioned in [15,16,18] but somewhat consistent with those reported in [12,17,19]. For 2024, the probability of aircraft being impacted by fragments capable of causing a catastrophic failure varied between 3×10^{-5} (LIN2 600) and 7×10^{-5} (LIN1 All), corresponding to an average collision rate of one airplane struck approximately every 30,000 and 14,000 years, respectively. For commercial aircraft passengers, still in 2024, the collective casualty probability ranged from 0.42% (LIN2 600) to 0.84% (LIN1 All), while the individual casualty probability varied between about 9×10^{-13} (LIN2 600) and 2×10^{-12} (LIN1 All). Therefore, also for commercial aircraft and passengers, the hazards due to uncontrolled reentries are still very small, even though in 2024 the risk figures were between 3 and 4 times higher than those found for 2019, despite the fact that the number of flights and passengers was virtually identical in those two years.

It should also be remarked that, always in 2024, the collective and individual casualty probabilities for aircraft passengers were still smaller than those for people on the ground by one order of magnitude. Thus, considering all the uncertainties involved, the overall global risk – including commercial aircraft – can still be calculated using the procedure recommended by the NASA standard [3] for people on the ground. However, a fatal impact involving an airliner, although much less likely, would be of a very different nature than a lethal impact on the ground. While a ground impact might typically affect one or a few people, in the case of an airplane the victims could number as many as a hundred or more, making such an event catastrophic. It is, therefore, reasonable to assume that somewhat lower and more conservative attention and warning thresholds should be adopted for aircraft than those established for ground hazards due to uncontrolled reentries.

In conclusion, although still small in absolute and relative terms, the risks presented by the surviving fragments of orbital objects reentering the atmosphere without control are rapidly growing, driven by the boom of the new space economy. To mitigate and control this risk, for people on the ground and airplanes in the air, it is necessary to act immediately before further and mighty growth in space activities materializes. Already, commercial air operations are being increasingly disrupted by uncontrolled reentries [18,19], and the costs have so far been absorbed by airlines, passengers, and the civil aviation system. But this cannot continue for much longer. As soon as possible, controlled reentries in designated safe areas should be adopted as a general rule for all spacecraft and orbital stages not able to demise completely.

6 ACKNOWLEDGMENTS

The activity presented in this paper was carried out in the framework of the ASI-PoliMi agreement No. 2023-37-HH.0 on "Technical and Scientific Activities to Support CSSA/ISOC and Simulation of Sensor Architectures for SST", and of the ASI-INAF agreement No. 2023-50-HH.0 on "Space Debris and Sustainability of

Long-Term Space Activities". The authors would also like to thank the US Space Track Organization for the catalog of the reentered objects, and the ESA DISCOS Database for the masses of spacecraft and orbital stages.

7 REFERENCES

1. Range Commanders Council, Range Safety Group Risk Committee (2023). *Common Risk Criteria Standards for National Test Ranges: Supplement*, Standard 321-23, Published by Secretariat, Range Commanders Council, US Army White Sands Missile Range, New Mexico.
2. Cole, J.K., Young, L.W. & Jordan-Culler, T. (1997). *Hazards of Falling Debris to People, Aircraft, and Watercraft*, Sandia Report SAND97-0805-UC-706, Sandia National Laboratories, Albuquerque, New Mexico.
3. NASA (2021). *Process for Limiting Orbital Debris*, NASA Technical Standard NASA-STD-8719.14C, National Aeronautics and Space Administration, Washington (DC).
4. US Government (2019). *Orbital Debris Mitigation Standard Practices*, Washington (DC).
5. Steering Group & Working Group 4 (2025). *IADC Space Debris Mitigation Guidelines*, Document IADC-02-01, Revision 4, Inter-Agency Space Debris Coordination Committee.
6. Space Debris Mitigation Working Group (2023). *ESA Space Debris Mitigation Requirements*, Document ESSB-ST-U-007, Issue 1, European Space Agency.
7. Safety and Mission Assurance Department (2023). *Space Debris Mitigation Standard*, Document JMR-003E (E), Japan Aerospace Exploration Agency.
8. Pardini, C. & Anselmo, L. (2022). The Kinetic Casualty Risk of Uncontrolled Re-entries Before and After the Transition to Small Satellites and Mega-constellations. *J. Space Saf. Eng.* **9**, 414–426.
9. Space Debris Mitigation Working Group (2023). *ESA Space Debris Mitigation Compliance Verification Guidelines*, Document ESSB-HB-U-002, Issue 2, European Space Agency.
10. Space Debris Mitigation Working Group (2015). *ESA Space Debris Mitigation Compliance Verification Guidelines*, Document ESSB-HB-U-002, Issue 1, European Space Agency.
11. Anselmo, L. & Pardini, L. (2005). Computational Methods for Reentry Trajectories and Risk Assessment. *Adv. Space Res.* **35**, 1343–1352.
12. Pardini, C. & Anselmo, L. (2013). Reentry Predictions for Uncontrolled Satellites: Results and Challenges. In *Proc. of the 6th IAASS Conference "Safety is Not an Option"*, ESA SP-715, European Space Agency, Noordwijk, The Netherlands.
13. Wilde, P. (2024). Aircraft Safety and Space Vehicle Hazards: How Safe from Space Debris Hazards Will Your Future Flights Be? In *Proc. of the 75th International Astronautical Congress*, International Astronautical Federation, Paper AA-24-D6.1.10.
14. Ailor, W. & Wilde, P. (2008). Requirements for Warning Aircraft of Reentering Debris. In *Proc. of the 3rd IAASS Conference "Building a Safer Space Together"*, ESA SP-662, European Space Agency, Noordwijk, The Netherlands.
15. Patera, R.P. (2008). Risk to Commercial Aircraft from Reentering Space Debris. In *Proc. of the AIAA Atmospheric Flight Mechanics Conference and Exhibit* (Honolulu, Hawaii), American Institute of Aeronautics and Astronautics, Paper AIAA 2008-6891.
16. Ailor, W. (2019). Hazards of Reentry Disposal Satellites from Large Constellations. *J. Space Saf. Eng.* **6**, 113–121.
17. Federal Aviation Administration (2023). *Report to Congress: Risk Associated with Reentry Disposal of Satellites from Proposed Large Constellations in Low Earth Orbit*, Department of Transportation, Washington (DC).
18. Hook, C., Wright, E., Byers, M. & Boley, A. (2024). Uncontrolled Reentries of Space Objects and Aviation Safety. *Acta Astronaut.* **222**, 69–80.
19. Wright, E., Boley, A. & Byers, M. (2025). Airspace Closures Due to Reentering Space Objects. *Sci. Rep.* **15**(1):2966.
20. Larson, E. (2013). Air-Space Traffic Interface Management. In *Safety Design for Space Operations* (Eds. F.A. Allahdadi, I. Rongier, P.D. Wilde & T. Sgobba), Butterworth-Heinemann, Elsevier, Oxford, United Kingdom, pp. 777–794.
21. Bellucci, A., Fuentes, N., Guerra-Algaba, M., Cointe-Fourrier, M. & Goester, J.F. (2017). Risk Analysis Between Aircraft and Space Debris During Atmospheric Reentry. In *Proc. of the 9th IAASS Conference "Know Safety No Pain"*, International Association for the Advancement of Space Safety, pp. 433–438.
22. Statista (2024). *Number of Flights Performed by the Global Airline Industry from 2004 to 2023, with Forecast to 2024*, https://www.statista.com/statistics/564769/airline-industry-number-of-flights/